

# Comparaison de la sévérité de normes utilisées pour les tests de vibration de luminaires

## Comparison of the Severity of Standards Used for the Vibration Testing of Luminaires

Frédéric Marin, Jean-Claude Golinval, Christian Marville\*, Arlette Blochouse\*  
Université de Liège, \*R-Tech (Schröder Group GIE) - Liège (Belgique)

### Résumé

Au cours de leur vie, les appareils d'éclairage routier (ou luminaires) sont soumis à des excitations environnementales induites par le trafic et le vent. Les phénomènes de fatigue engendrés par les vibrations ambiantes de longue durée sont la cause principale des ruptures dans les luminaires montés sur poteau. Les fabricants d'appareils d'éclairage routier sont concernés au plus haut point par les tests de vibration de leurs prototypes afin de déterminer s'ils peuvent supporter, sans être endommagés, l'environnement vibratoire auquel ils sont soumis durant leur vie. Jusqu'à présent, les tests de qualification sont réalisés selon différentes normes qui ne sont pas spécifiques aux appareils d'éclairage routier. Ces normes n'ont pas la même sévérité de sorte que le choix de l'une plutôt qu'une autre n'est pas bien défini.

L'objectif de la recherche présentée ici est de proposer une nouvelle méthode pour quantifier la sévérité de différents environnements vibratoires. Pour cela, différents critères de sévérité sont d'abord définis : ils sont basés sur le spectre de robustesse, le spectre de dommage par fatigue et le spectre d'énergie dissipée. Grâce à ces critères, la sévérité de différentes normes comme IEC 68-2-6, ANSI C 136-31, ... peut être estimée et comparée. Afin de choisir le critère le plus approprié, l'identification et la connaissance des processus de rupture sont de première importance. Comme illustration, la méthode est appliquée au cas simple d'une poutre excitée par la base. Les tests de vibration sont réalisés au moyen d'un excitateur électrodynamique dans le but de valider l'approche théorique.

### Abstract

*During their lifetime, street lighting devices (or luminaires) are subject to environmental excitations induced by the traffic and the wind. Fatigue effects due to ambient vibrations of long duration are the main cause of structural failures in outdoor pole mounted luminaires. Street lighting manufacturers are very much concerned with vibration testing of luminaire prototypes in order to determine if they can support the vibration environment expected during their lifetime without being damaged. Up to now, qualification tests are performed according to different standards which are not specific to street lighting devices. These standards do not have the same severity so that the choice of one standard rather than another is not obvious.*

*The aim of the research presented here is to propose a new methodology to quantify the severity of different vibration environments. To this end, different severity criteria are first defined : these are based on the maximax response spectrum, the fatigue damage spectrum or the dissipative damage spectrum. Based on these criteria, the severity of different standards such as IEC 68-2-6, ANSI C 136-31, ... may be estimated and compared. To choose the most appropriate criterion, the identification and the knowledge of failure processes are of prime importance. As an example, the methodology is applied to the simple case of a base excited beam. Vibration testing is performed on an electro-dynamic shaker to validate the theoretical approach.*

## 1. INTRODUCTION

The objective of the paper is to present a methodology to quantify the severity of vibration environments. The first step consists in reviewing the possible standards used for the vibration testing of luminaires such as the International Electrotechnical Commission IEC 68-2-6 and the American National Standard for Roadway Lighting ANSI C 136-31.

The second step deals with the definition of severity criteria built on a base excited one degree of freedom reference system : maximax response spectrum, fatigue damage spectrum or dissipative damage spectrum. To choose the most appropriate criterion, the identification and knowledge of failure processes are of prime importance. The generalisation of fatigue damage spectrum computation to multi-degree-of-freedom systems is also presented. The methodology uses the stress time response provided by a finite element model to compute damage using a cycle counting method (rainflow).

Finally, the methodology is validated on the example of a clamped beam submitted to vibration testing on an electro-dynamic shaker. Stress measurements are obtained by means of strain gauges and the damage is also computed using the rainflow method.

## **2. VIBRATION TESTING OF LUMINAIRES**

During their lifetime, street lighting devices are subject to environmental excitations induced by the traffic and the wind. Fatigue effects due to ambient vibrations of long duration are the main cause of structural failures in outdoor pole mounted luminaires.

Street lighting manufacturers are very much concerned with vibration testing of luminaire prototypes in order to determine if they can support the vibration environment expected during their lifetime without being damaged [1]. Up to now, qualification tests are performed according to different standards which are not specific to street lighting devices. These standards do not have the same severity so that the choice of one standard rather than another is not obvious.

<b>Standard</b>	<b>Excitation</b>	<b>Amplitude</b>	<b>Duration</b>
<b>IEC 68-2-6</b>	sine sweep	0.15 mm	100
	[10-55-10] Hz	fixing point	sweeps
<b>ANSI C 136-31</b>	sine	1.5 (3) g	100 000
	$f_0 \in [5-30]$ Hz	centre of gravity	cycles

**Table 1 : Possible standards and parameters for the vibration testing of luminaires**

### **2.1. The International Electrotechnical Commission IEC 68-2-6 Standard**

This standard describes a testing method applicable to components, equipment and other articles which, during transportation or in service, may be subjected to conditions involving vibration of a harmonic pattern, generated primarily by rotating, pulsating or oscillating forces, such as occur in ships, aircraft, land vehicles, rotorcraft and space applications or are caused by machinery and seismic phenomena [2]. It consists basically of submitting a specimen to sinusoidal vibration over a given frequency range or at discrete frequencies for a given period of time. The object of the standard is to provide a standard procedure to determine the ability of components, equipment and other articles to withstand specified severities of sinusoidal vibration. It is emphasised that vibration testing always demands a certain degree of engineering judgement, and both the supplier and purchaser should be fully aware of this fact. The main part of this standard deals primarily with the methods of controlling the test at specified points, and gives, in detail, the testing procedure. The requirements for the vibration motion, choice of severities including frequency ranges, amplitudes and endurance times are also specified; these severities representing a rationalised series of parameters. The relevant specification writer is expected to choose the testing procedure and values appropriate to the specimen and its use. Today, one can find some data and indications in previous proposals.

Some 26 years ago, introduction of vibration tests in the IEC 60598 standard [3] (Luminaires - General requirements and tests) has been discussed by IEC Experts Working Group LUMEX. This resulted in a project with two options : a first procedure aligning with IEC 68-2-6, reproducible and therefore suitable for possible introduction in a standard and a second procedure making use of a specific testing equipment like a shaking machine, simple but less reproducible than the first procedure. At the Brussels meeting (1977) of IEC-Technical Committee N°. 34 (lamps and related equipment)-Sub-committee 34D (luminaires), it was decided to keep the proposal at the Secretariat stage for information only.

In the above options, the first proposal suggested that :

- in view of the difficulties of rigorously defining resonance, an endurance test should be made by sweeping over a sinusoidal frequency range (a random vibration test is considered unnecessarily sophisticated for the luminaires covered by the specification);
- definitions and values for the various parameters should be taken from IEC Publication 68-2-6;
- short and rigid mounting piece should be used such that no resonance of this mounting piece (without luminaire) should occur within 150 % of the maximum test frequency;
- the control point should be as close as possible to the fixing point;
- the sweep rate should be one octave per minute;
- the test should be performed along each structural axis.

In 1998, the introduction of a specific vibration test for rough service luminaires in the IEC standard 60598 was voted by the International Electrotechnical Commission. It means specific requirements for luminaires used in rough environment situations such as engineering workshops, building sites and similar applications.

The vibration requirements are :

- a test is made by sweeping over the sinusoidal frequency range [10-55-10] Hz;
- the imposed displacement must be constant and equal to 0.35 mm;
- the duration of the endurance test is 30 minutes;
- the sweep rate is one octave per minute;
- the test must be performed along the most onerous direction.

Taking into account the different remarks mentioned in this paragraph, an example of test following IEC 68-2-6 requirements is given in Table 1.

## **2.2. The American National Standard for Roadway Lighting ANSI C 136-31 Standard**

The USA ANSI C 136-31 new standard (2001) proposes that a requirement for a minimum vibration withstand capability be considered for luminaires for road and street lighting. According to the proposal, there are factors that may cause externally induced vibration effects but which may not be adequately covered by the application of a static load test. For this reason, a vibration test might serve as a more appropriate and suitable substitute. This ANSI Standard will probably be included in the new CANENA Luminaire Standard that will harmonise Canadian, U.S. and Mexican requirements.

This new standard suggests that :

- the fundamental resonant frequency must be determined for each of the three perpendicular planes and must be between 5 and 30 Hz;
- the luminaire must be vibrated at or near his natural frequency;
- the acceleration intensity measured at the luminaire centre of gravity must be 1.5 g for normal roadway applications and 3 g for bridge and overpass applications;
- the lighting device must be capable of withstanding the described vibration for 100 000 cycles in each plane.

Table 1 summarises the standards used for the vibration testing of luminaires.

## **3. SEVERITY OF VIBRATION ENVIRONMENTS**

Three basic criteria are available in the literature to quantify the severity of a vibration environment [4], [5] :

- the maximax response spectrum, associated with the maximum relative displacement representative of the maximum stress in the equipment;
- the fatigue damage spectrum, which is related to the deterioration of the material when submitted to repeated stresses;
- the dissipative damage spectrum, based on the assumption that the energy dissipated by the equipment is correlated with the severity of the vibration environment.

Since fatigue effects of long time ambient vibration are the leading cause of structural failures in outdoor pole mounted luminaires, the most representative criterion is the fatigue damage spectrum.

In the frequency range of interest [10-55] Hz, measurement results show that only the first mode shape of the luminaire is generally excited. For this reason, the definition of severity criteria is based on the application of the vibration excitation to the base of a reference one-degree-of-freedom system. The generalisation of fatigue damage spectrum computation to multi-degree-of-freedom systems is also presented.

### **3.1. Reference One-degree-of-freedom System**

The equation of movement of the reference system shown in Figure 1 is given by

$$\ddot{z} + 2 \varepsilon \omega_0 \dot{z} + \omega_0^2 z = -\ddot{x} \quad (1)$$

where  $x(t)$  describes the motion imposed to the base,  $z(t)$  the relative position of the mass,  $\varepsilon$  the damping ratio and  $\omega_0$  the natural pulsation of the system. The mass  $m$ , stiffness  $k$  and damping  $c$  are the parameters of a modal model of the luminaire obtained either by finite element analysis or by experimental modal identification.

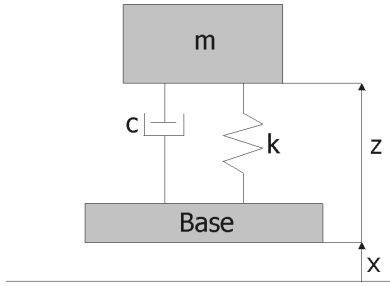


**Figure 1 : Reference 1-dof-mass-spring-damper system**

For a given vibration environment  $x(t)$ , the maximal response  $Z_{\max}$  of the relative displacement is a function of the natural frequency  $f_0$  of the system and of the damping ratio  $\varepsilon$ . For a stress level  $\sigma_i$ , the corresponding damage  $d_i$  is defined by

$$d_i = \frac{n_i}{N_i} \quad (2)$$

where  $n_i$  is the number of cycles of amplitude  $\sigma_i$  and  $N_i$  the maximum number of cycles before deterioration at the same stress level.  $N_i$  is given by the classical Wöhler curves of the material, which in their central part, can be approximated by Basquin's relationship :

$$N_i \sigma_{i,\max}^b = A^b \quad (3)$$

where  $b$  and  $A$  are two material dependant parameters. If one assumes a linear behaviour of the material, stress and relative displacement may be related by a coefficient  $K$  :

$$\sigma_{i,\max} = K Z_{i,\max} \quad (4)$$

According to Miner's linear cumulative damage law and using equations (3) and (4), one obtains the total damage  $D$  corresponding to the reference 1-dof system in the form

$$D = \left(\frac{K}{A}\right)^b \sum_i n_i Z_{i,\max}^b(f_0, \varepsilon) \quad (5)$$

The fatigue damage spectrum is the curve which represents the total damage  $D$  as a function of the natural frequency  $f_0$ , for a given  $\varepsilon$ . Consequently, the comparison between two vibration environment will be centred on the assumption that two environments have the same severity if they induce the same damage to the reference 1-dof system.

The localisation in the structure of the maximal stress needs the use of a more elaborate finite element model or of an experimental model with strain gauges.

For a sinusoidal excitation at discrete frequency (ANSI C 136-31 standard) or a logarithmic sine sweep excitation (IEC 68-2-6 standard), the expected value of  $Z_{i,\max}$  may be easily calculated.

### 3.1.1. Sinusoidal Excitation at Discrete Frequency

In the case of a sinusoidal excitation at discrete frequency, the excitation time history follows a relationship of the form

$$\ddot{x}(t) = \ddot{X}_{\max} \sin(\omega t + \phi) \quad (6)$$

where  $\ddot{X}_{\max}$  is the constant peak amplitude,  $\omega$  the excitation pulsation and  $\phi$  the phase angle.

Making the assumption of a permanent sinusoidal response, the maximal relative displacement is given by

$$Z_{\max} = \frac{\omega^\alpha \beta_{\max}}{\omega_0^2 \sqrt{(1-h^2)^2 + \frac{h^2}{Q^2}}} \quad (7)$$

$$\text{with } \begin{cases} h = f/f_0 \\ Q = 1/2 \varepsilon \\ \alpha = 0 \text{ if } \beta_{\max} = \ddot{X}_{\max} \\ \alpha = 1 \text{ if } \beta_{\max} = \dot{X}_{\max} \\ \alpha = 2 \text{ if } \beta_{\max} = X_{\max} \end{cases}$$

The number of cycle of period T and frequency f corresponding to a test of duration  $t_b$  can be written as

$$n_i = \frac{t_b}{T} = f t_b \quad (8)$$

From equations (5), (7) and (8), the total damage D corresponding to the reference 1-dof system subject to a sinusoidal excitation at discrete frequency is finally rewritten as

$$D = \left(\frac{K}{A}\right)^b f t_b \frac{\omega^{\alpha b} \beta_{\max}^b}{\omega_0^{2b} \left[ (1-h^2)^2 + \frac{h^2}{Q^2} \right]^{\frac{b}{2}}} \quad (9)$$

### 3.1.2. Logarithmic Sine Sweep Excitation

In the case of a logarithmic sine sweep excitation, the excitation time history is generally made of several excitation levels which follow a relationship of the form

$$\ddot{x}_i(t) = \ddot{X}_{i,\max} \sin(\omega(t)t + \phi) \quad i: 1 \rightarrow L \quad (10)$$

where  $\ddot{X}_{i,\max}$  is the constant peak amplitude of excitation level i,  $\omega(t)$  the time dependant excitation pulsation and L the total number of excitation levels.

Making the assumption of a sufficiently low sweep rate to consider for each excitation frequency a permanent response, the logarithmic sweep is defined by

$$f(t) = f_1 e^{\frac{t}{T_1}} \quad \text{with } T_1 = \frac{t_b}{\ln(f_2/f_1)} \quad (11)$$

where  $[f_1, f_2]$  and  $t_b$  define respectively the frequency range and the duration to sweep this interval.

From equations (5), (7) and (11), the total damage D corresponding to the reference 1-dof system subject to a sine sweep excitation is finally rewritten as

$$D = \left(\frac{K}{A}\right)^b f_0 T_1 \omega_0^{(\alpha-2)b} \sum_i \left[ \beta_{i,\max}^b \int_{h_i}^{h_{i+1}} \frac{h^{\alpha b}}{\left[ (1-h^2)^2 + \frac{h^2}{Q^2} \right]^{\frac{b}{2}}} dh \right] \quad (12)$$

## 3.2. Generalisation to Multi-degree-of-freedom systems

As previously mentioned, the localisation in the structure of the maximal stress is not possible with the simplified one-degree-of-freedom model. To this end, a more elaborated finite element model taking into account the geometry of the structure needs to be used. Figure 2 summarises the different steps constituting the general methodology for the computation of fatigue damage.

Two important parts can be emphasised :

- the finite element analysis;
- the cycle counting process.

**3.2.1. Finite Element Analysis**

The starting point of the methodology is the finite element modelling of the structure. A dynamic analysis solves the following homogeneous equation system

$$\mathbf{M} \ddot{\mathbf{x}} + \mathbf{K} \mathbf{x} = 0 \tag{13}$$

providing the modal parameters : natural frequencies  $f_0^{F.E.}$  and mode shapes  $\Theta^{F.E.}$ .  $\mathbf{M}$  and  $\mathbf{K}$  are respectively the mass and stiffness matrices. The vector  $\mathbf{x}$  represents, in structural axes, the displacement associated with each degree of freedom of the finite element model. A comparison of the computed modal parameters with the ones identified by an experimental modal analysis allows to verify the quality of the modelling and to update it if necessary. The experimental modal analysis is also necessary to estimate the modal damping ratios.

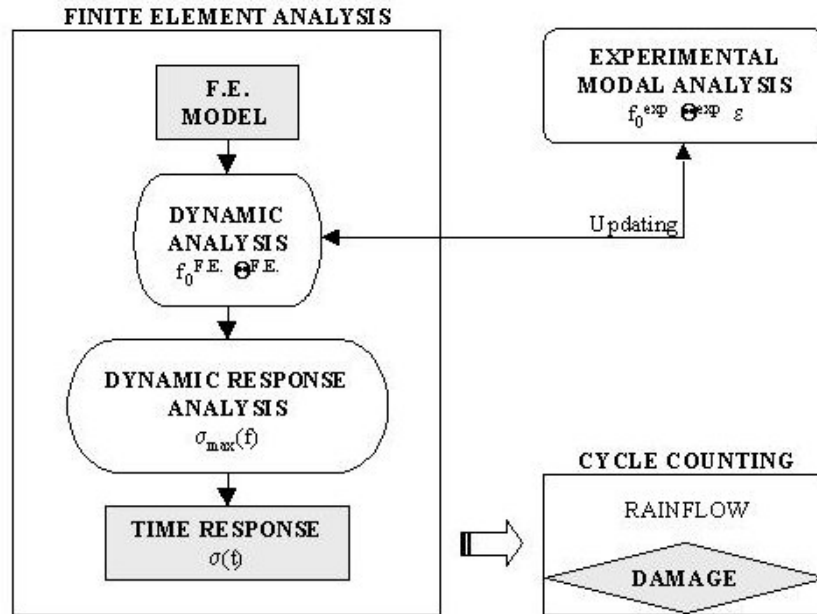


**Figure 2 : General methodology for the computation of fatigue damage**

The linear vibrations of a base excited structure are governed by the differential equation system given by

$$\mathbf{M} \ddot{\mathbf{x}} + \mathbf{C} \dot{\mathbf{x}} + \mathbf{K} \mathbf{x} = \mathbf{p} \tag{14}$$

where  $\mathbf{C}$  is the damping matrix and  $\mathbf{p}$  a vector which represents the structural forces acting on each degree of freedom of the interface. The supposed elastic linear behaviour of the structure easily allows to solve the problem in the frequency domain providing as response the maximal stress observed in one element during one cycle at the excitation frequency  $f$ .

The last step of the finite element analysis consists in generating the stress time history from the results obtained in the frequency domain. Making the assumption that an harmonic excitation induces an harmonic response, the expression of the stress time history can be written as

$$\sigma(t) = \sigma_{\max}(f) \cos(2\pi ft) \tag{15}$$

In the case of a logarithmic sine sweep excitation, equation (15) is associated with equation (11) to relate the frequency history to the time.

Once the stress time history is known, the damage is computed by a cycle counting process.

**3.2.2. Cycle Counting Process**

In equation (3), describing Basquin’s relationship, it is suppose that the specimen is subject to a sinusoidal alternated load of constant amplitude which induces a stress  $\sigma_{i,\max}$  showing the same characteristics. Experimental observations have shown that when a positive static stress  $\sigma_m$  is added to the sinusoidal alternated stress  $\sigma_{i,\max}$ , the lifetime of the specimen decreases. The opposite effect is observed when a compressive mean stress is applied. Such a phenomenon is taken into account by a Haigh diagram [6] like the one shown in Figure 3. For a given lifetime  $N$ , the admissible alternated stress  $\sigma_{i,\max}$  is expressed according to the mean stress  $\sigma_m$ .

The Haigh diagram allows to transform each mean non-zero stress cycle  $\sigma_m$  of amplitude  $\sigma_{i,max}$  into a mean zero stress cycle of amplitude  $\sigma_a$ . For example, the cycle  $(\sigma_m, \sigma_{i,max})$  represented by point B is equivalent from a lifetime point of view to the cycle  $(0, \sigma_a)$  represented by point A.

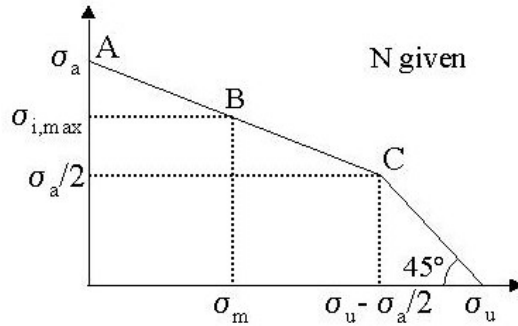


**Figure 3 : Example of a Haigh diagram**

Knowing that the Haigh diagram is made of two linear parts intersecting at point C  $(\sigma_u - \sigma_a/2, \sigma_a/2)$ , where  $\sigma_u$  is the failure limit of the material, it is possible to express  $\sigma_a$  in terms of  $\sigma_m$ ,  $\sigma_{i,max}$  and  $\sigma_u$  as

$$\sigma_a = \sigma_u + \frac{1}{2}(\sigma_{i,max} - \sigma_m) - \sqrt{\left(\sigma_u + \frac{1}{2}(\sigma_{i,max} - \sigma_m)\right)^2 - 2\sigma_{i,max}\sigma_u} \quad (16)$$

Equation (3) can be rewritten as

$$N_i \sigma_a^b = A^b \quad (17)$$

This procedure is equivalent to modifying the Wöhler curve for each mean non-zero stress cycle : the decrease in lifetime induced by a positive static stress is represented by a lowering of the initial Wöhler curve.

Considering the Haigh diagram at the endurance limit, a second procedure consists in directly writing the modified endurance limit  $\sigma_e$  according to  $\sigma_m$ ,  $\sigma_u$  and the endurance limit for a mean zero stress cycle  $\sigma_e^0$  to obtain

$$\sigma_e = \begin{cases} -\sigma_e^0 \sigma_m / (2\sigma_u - \sigma_e^0) + \sigma_e^0 & \text{if } \sigma_m \leq (\sigma_u - \sigma_e^0/2) \\ \sigma_u - \sigma_m & \text{if } \sigma_m > (\sigma_u - \sigma_e^0/2) \end{cases} \quad (18)$$

In this case, the modified Wöhler curve is

$$N_i \sigma_{i,max}^b = A^b \left( \frac{\sigma_e}{\sigma_e^0} \right)^b \quad (19)$$

In order to decompose the stress time history provided by the finite element analysis into elementary cycles of known amplitude and average, the use of a cycle counting process is necessary. As shown in Figure 4, the rainflow method implemented uses four successive points of the stress time history to identify one cycle which in the stress-strain plane corresponds to a closed hysteresis loop [6], [7], [8].

The decomposition of the stress time history is performed in several steps :

- the signal is reduced into a sequence of local maxima and minima;
- the first four successive points  $\sigma_1, \sigma_2, \sigma_3, \sigma_4$  are examined and three lengths are computed :  $\Delta\sigma_1 = |\sigma_2 - \sigma_1|$ ,  $\Delta\sigma_2 = |\sigma_3 - \sigma_2|$ ,  $\Delta\sigma_3 = |\sigma_4 - \sigma_3|$ ;
- if  $\Delta\sigma_2 \leq \Delta\sigma_1$  and  $\Delta\sigma_2 \leq \Delta\sigma_3$ , the rainflow cycle defined by the couple  $(\sigma_2, \sigma_3)$  is identified : its amplitude is defined by  $\sigma_{i,max} = |\sigma_3 - \sigma_2|/2$  and its mean value by  $\sigma_m = |\sigma_3 + \sigma_2|/2$ ;  $(\sigma_2, \sigma_3)$  is eliminated from the signal and  $\sigma_1$  linked to  $\sigma_4$ ;
- otherwise, the rank of the four points is incremented of one unity and the previous test is applied;
- the process is repeated up to the last point of the sequence of local maxima and minima.

After completion of these different steps, several non-extracted points remain. They make up the residue constituted by an increasing and after decreasing signal. The maximum and minimum of the initial sequence are included in the

residue forming the most important length observed in the sequence. The contribution of the residue to the damage may therefore not be neglected. That is why the residue must also be broken down into elementary cycles. To this end, a new sequence is built up on two residues one after the other. New cycles are then extracted applying the counting process.

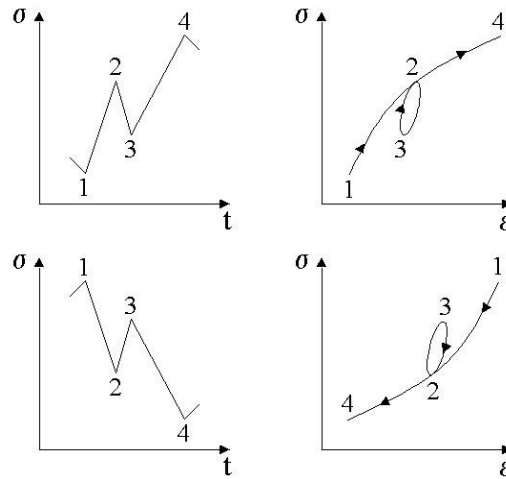


**Figure 4 : Definition of a rainflow cycle**

Practically, only a discrete number of amplitude classes is taken into account. Each rainflow cycle ( $\sigma_k, \sigma_l$ ) is stocked in a rainflow matrix R. The damage computation from the rainflow matrix R is easily performed using equations (2) and (16), (17) or (18), (19).

#### 4. APPLICATION EXAMPLE

The developed methodology is illustrated on the simple case of a base excited beam supporting, as shown in Figure 5, a concentrated mass at its free end ( $M_a=4.77$  kg,  $r=0.04$  m). The structure is made up of steel ( $A=886$  MPa,  $b=7$ ,  $\sigma_u=415$  Mpa,  $\sigma_e^0=128$  Mpa, Young modulus  $E=205 \cdot 10^3$  Mpa, density  $\rho=7850$  kg/m<sup>3</sup>) and four different lengths are considered ( $L=0.575, 0.510, 0.475$  and  $0.445$  m). The section of the beam is rectangular ( $b_s=0.08$  m,  $h_s=0.015$  m).

Equation (4) has shown that the methodology based on the reference one-degree-of-freedom system requires the knowledge of the coefficient K relating the stress to the relative displacement. To this end, an analytical approach has been used to compute K.

The general methodology centred on a finite element analysis is applied to a 3D volumic model of the beam. Vibration testing performed on an electro-dynamic shaker allows to validate the theoretical approaches. Stress measurements are obtained by means of strain gauges and the damage is computed using the rainflow counting process.

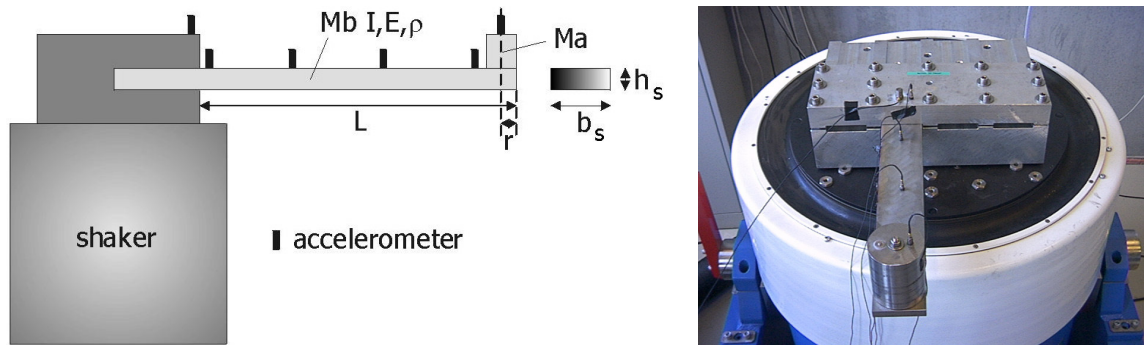


**Figure 5 : Experimental test-case mounted on an electro-dynamic shaker**

The developed theory requiring a response computation has highlighted that both methodologies are subject to the same important unknown i.e., the damping ratio  $\varepsilon$ . In order to estimate this modal parameter, an experimental modal analysis has been first performed.

**4.1. Modal Parameter Identification**

The modal parameters are identified using the Frequency Response Functions (FRF) measured during the different tests. The magnitude of such a function computed between the fixing point and the free end of the beam is shown in Figure 6.

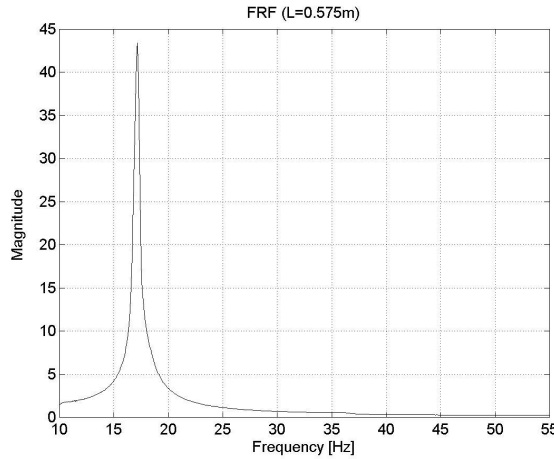


**Figure 6 : FRF measured during the test following IEC 68-2-6 standard**

It clearly appears that in the frequency range of interest [10-55] Hz, the behaviour of the structure may be approximated by a one-degree-of-freedom system (the peak represents the first bending mode shape of the beam). Based on this assumption, the damping ratio is given by

$$Q = \frac{f_0}{\Delta f} \Big|_{\frac{|H|_{\max}}{\sqrt{2}}} \approx \frac{1}{2\varepsilon} \tag{20}$$

and the results are summarised in Table 2. The modal tests reveal that both the frequencies and damping ratios are subject to the amplitude level. Such a phenomenon is a characteristic of non-linear structures. The most plausible explanation is to admit that clamping is not perfect : its properties vary with the severity of the test. The identified damping ratios will nevertheless be used in the different damage computation methodologies.

L [m]	ANSI C 136-31 (roadway)		IEC 68-2-6	
	f <sub>0</sub> [Hz]	ε [%]	f <sub>0</sub> [Hz]	ε [%]
0.575	17.1	0.37	16.9	1.24
0.510	20.2	0.79	20.0	1.40
0.475	22.5	0.69	21.9	2.29
0.445	24.8	1.26	24.1	3.42

**Table 2 : Results of the modal parameter identification**

**4.2. Reference One-degree-of-freedom System**

The first step consists in finding the analytical expression of coefficient K in the particular case of a beam with a mass at its free end. At the clamping, the maximal stress is given by

$$\sigma = \frac{M \frac{h_s}{2}}{I} \quad (21)$$

where  $I$  is the inertia of the section and  $M$  the torque at the clamping which can be expressed in terms of the beam deflection  $v(x)$  as

$$M = E I \frac{d^2 v(x)}{dx^2} \quad (22)$$

The deflection is a function varying along the beam with the parameter  $x$  [9] and is maximal at the free end where it is equal to the relative displacement  $Z$

$$v(x) = \left[ \frac{x^3}{L^3} - 3 \frac{x}{L} + 2 \right] \frac{Z}{2} \quad (23)$$

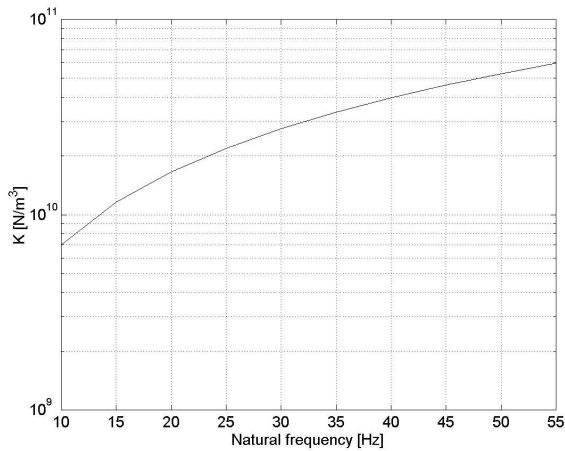
Note that the function of  $x$  in brackets is the first bending mode shape of the beam. Finally, from equations (21), (22) and (23), the analytical expression of coefficient  $K$  becomes

$$K = \frac{3 E h_s}{2 L^2} \quad (24)$$

showing that for given material and section,  $K$  only depends on the length of the beam which can be related to the first natural frequency [9] by

$$0.24 \rho b_s h_s L^4 + Ma L^3 - \frac{3 E I}{\omega_0^2} = 0 \quad (25)$$

The evolution of coefficient  $K$  with the natural frequency of the structure is shown in Figure 7 and given in Table 3 for the four considered lengths of the beam.



L [m]	f <sub>0</sub> [Hz]	K [N/m <sup>3</sup> ]
0.575	17.4	1.32E10
0.510	21.1	1.62E10
0.475	23.7	1.87E10
0.445	26.2	2.04E10

**Table 3 : Results of the analytical approach**

**Figure 7 : Evolution of coefficient  $K$  with  $f_0$**

The difference in natural frequencies between Table 2 and Table 3 is due to the simplifying assumptions of the analytical model :

- the mass  $Ma$  is concentrated at the end of the beam but it is not really true for the experimental test-case ( $r=0.04$  m);
- perfect clamping is considered.

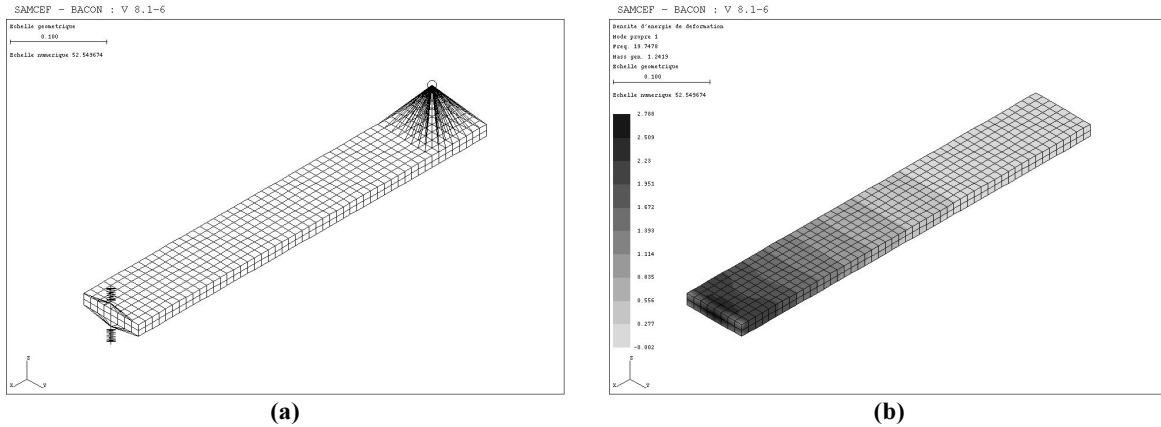
### 4.3. General Methodology

The properties of the finite element model used for the damage computation are the following :

- the model is made up of 3D volumic shell elements;
- the mass  $Ma$  is concentrated at its centre of gravity;

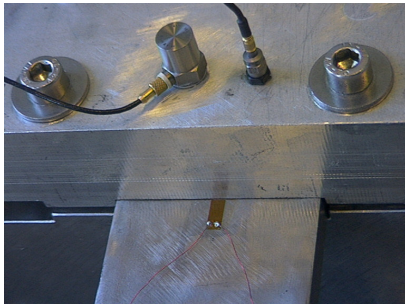
- the clamping is modelled by spring elements;
- the model is updated on the first natural frequency.

Figure 8 shows the 3D volumic finite element model of the beam and the strain energy density map associated with the first bending mode shape. Such an iso-strain map highlights the critical areas (i.e., the clamping in the case of the present structure) where strain gauges should be placed to measure the maximal stress. For this reason, the finite element model is a precious aid to the positioning of strain gauges.



**Figure 8 : (a) 3D volumic finite element model - (b) Strain energy density (1<sup>st</sup> mode shape)**

A view of the experimental set-up is given by Figure 9. The natural frequencies of the updated model are summarised in Table 4.



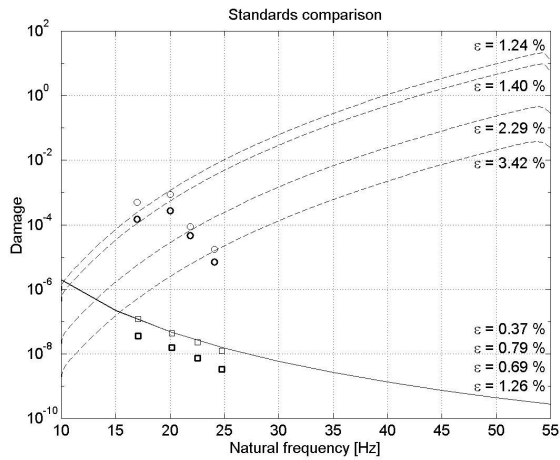
**Figure 9 : Strain gage positioned at the clamping**

L [m]	ANSI C 136-31 (roadway)	IEC 68-2-6
	f <sub>0</sub> [Hz]	f <sub>0</sub> [Hz]
0.575	17.0	17.0
0.510	20.0	20.0
0.475	22.5	21.9
0.445	24.8	24.0

**Table 4 : Natural frequencies of the 3D F.E. model**

#### 4.4. Results comparison

The fatigue damage spectra resulting from the different computation methodologies and standards used for the vibration testing of luminaires are compared in Figure 10.



### Legend

IEC 68-2-6 standard

**dashed line** : 1dof/ $K_{analytic}$  method

**black circles** : general method

**bold circles** : measurement results

ANSI C 136-31 standard (1.5 g)

**solid line** : 1dof/ $K_{analytic}$  method

**black squares** : general method

**bold squares** : measurement results

**Figure 10 : Standards severity and comparison of damage computation methods**

The curves correspond to the reference one-degree-of-freedom system with the analytic computation of  $K$ . For a same standard, each curve represents the fatigue damage spectrum for a given damping ratio constant in the frequency range [10-55] Hz. It appears that the severity of the IEC 68-2-6 standard is function of the damping ratio which is not the case with the ANSI C 136-31 standard for small damping ratio ( $\epsilon < 10\%$ ). In the last case, the shaker control being performed at the centre of gravity of the structure, the ANSI C 136-31 standard will remain independent of the damping ratio until the base displacement may be considered small in comparison with the displacement at the centre of gravity. In the other case, the shaker control being performed at the fixing point, the response at the centre of gravity is conditioned by the damping ratio.

The circles and squares represent the results of computation and measurements for the four considered lengths of the beam. The same remarks can be formulated about the effect of the damping ratio on standards severity.

The comparison of measurement results with the computation results shows that the computation is conservative. The difference in stress belongs to the interval [4-20]%. The correlation between measurements and computations is better for the sine sweep excitation than for the sinusoidal excitation at the natural frequency. Several sources of error can be pointed out :

- One drawback of the developed methodologies is the dependence of the computed response on the damping ratio. A precise identification of the damping ratio is then of prime importance but, unfortunately, it is well-known that this task is very difficult to perform.

Stress measurements have been performed on the 0.575 length beam subject to a sinusoidal excitation of 0.5 g measured at the clamping. The estimated modal parameters are  $f_0 = 17.1$  Hz and  $\epsilon = 1.34\%$ . Different discrete excitation frequencies have been experimented : 25.2, 20.1 and 17.7 Hz. For the same damping ratio and excitation frequencies, computations have been made with the general methodology. The results are shown in Figure 11. When the excitation frequency is far away from the natural frequency, the error in stress between measurements and computations at location 1 (close to the clamping) is only 4%. If the excitation frequency is brought closer to the natural frequency, the error becomes 21% and is maximum at  $f_0$ . Close to the natural frequency, the identification of the damping ratio is of prime importance.

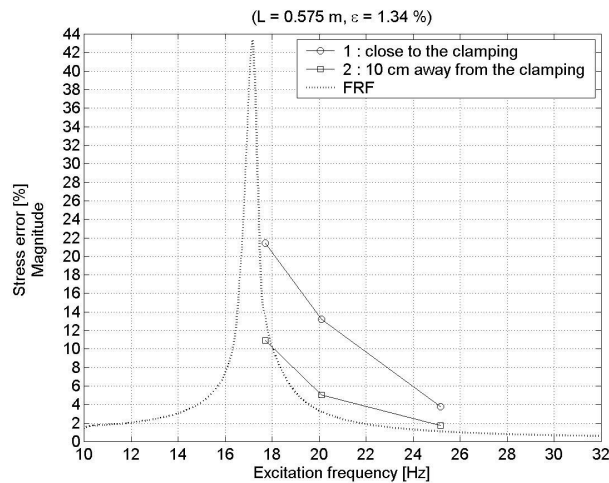


**Figure 11 : Effect of the excitation frequency and gauge positioning on the stress error**

- Figure 11 also highlights that the effect of stress gradients in critical areas can be important. The error in stress between measurements and computations at location 2 (10 cm away from the clamping) varies from 2 % (away from the natural frequency) to 11 % (close to the natural frequency). Between locations 1 and 2, the error in stress is divided by 2. A better accuracy between stress computations and measurements is obtained at locations where stress gradients are weak.
- Sinusoidal excitations at natural frequency are difficult to perform in practice. If the natural frequency is not identified with sufficient accuracy or slight changes occur during the test, the test severity may be completely different.
- The considered clamping model is very simple.

## 5. CONCLUSIONS

The developed methodologies are based on the fatigue damage spectrum criterion. The choice of this criterion among others has been imposed by the identification and knowledge of failure processes. The ability to know and compare the severity of the standards used in the vibration testing of street lighting devices is of prime importance for the luminaire manufacturer.

Before being applied to a real luminaire, the different methods have been tested on the simple case of a base excited beam supporting a mass at its free end. The results obtained by measurement and computation have shown that the one-degree-of-freedom system methodology is a good approach to predict the damage spectrum behaviour of a structure subject, for example, to a sinusoidal excitation (damping ratio effect, excitation frequency effect). If a more accurate damage computation is needed, a more elaborate finite element model is to be taken into account. When the excitation is away from the natural frequency, a very good correlation between strain gauge measurements and model is obtained. Unfortunately, most of the time the first natural frequency of the device is included in the excitation frequency range imposed by standards. In this case, the effect of the damping ratio is of primary importance and the error on the stress prediction may be high.

Other sources of error are the gauge positioning, the boundary conditions modelling, the difficulty to perform exactly a vibration test at the natural frequency (ANSI C 136-31), ...

## ACKNOWLEDGMENT

This research is funded by R-Tech (Schröder Group GIE) and the Walloon Region within the framework of the research convention 'First-Doctorat Entreprise n°991/4177'. They are gratefully acknowledged.

## REFERENCES

- [1] MARIN F., GOLINVAL J.C., MARVILLE C., *Accelerated Fatigue Testing Methodology of Luminaires on Electro-Dynamic Shaker*, Second International Conference on Advanced Computational Methods in Engineering, Liège (Belgium), May 28-31, 2002
- [2] INTERNATIONAL STANDARD IEC 68-2-6, *Environmental Testing – Part 2 : Tests – Test Fc : Vibration (sinusoidal)*, International Electrotechnical Commission, Sixth Edition, March 1995
- [3] INTERNATIONAL STANDARD IEC 60598-1, *Luminaires - General requirements and tests*, International Electrotechnical Commission, Fifth Edition, December 1999
- [4] NORME GAM-EG-13, *Essais généraux en environnement des matériels : annexe générale mécanique*, 1992
- [5] CAMBIER F., DEHOMBREUX P., VERLINDEN O., CONTI C., *Equivalence criteria between mechanical environments*, European Journal of Mechanical Engineering, Vol. 41 No. 4, 219-226, 1997
- [6] PITOISET X., *Méthodes spectrales pour une analyse en fatigue des structures métalliques sous chargements aléatoires multi-axiaux*, Thèse de doctorat, Université Libre de Bruxelles, 2001
- [7] DOWLING N. E., *Mechanical Behavior of Materials*, Engineering Methods for Deformation, Fracture and Fatigue, Prentice Hall, Second Edition, 1999
- [8] AMZALLAG C., GEREY J.P., ROBERT J.L. & BAHUAUD J., *Standardization of the rainflow counting method for fatigue analysis*, International Journal of Fatigue, 16(4) : 287-293, 1994
- [9] BLEVINS R. D., *Formulas for Natural Frequency and Mode Shape*, Van Nostrand Reinhold Company, 1979